Poly(vinyl alcohol) and Layered Double Hydroxide Composites: Thermal and Mechanical Properties

B. Ramaraj,[1] Sanjay K. Nayak,[2] Kuk Ro Yoon[3]

[1]*Research and Development Department, Central Institute of Plastics Engineering and Technology (CIPET), Ahmedabad 382 445, Gujarat, India*
[2]*Corporate Office, Central Institute of Plastics Engineering and Technology (CIPET), Guindy, Chennai 60032, Tamil Nadu, India*
[3]*Nano Bio-Sensor Research Team (BK21), Department of Chemistry, Hannam University, Yuseong-gu, Daejeon-305-811, Korea*

ABSTRACT: Nanocomposites of poly(vinyl alcohol) (PVA) with Mg-Al layered double hydroxides (LDHs) were prepared with different compositions, viz., 2, 4, 6, and 8 wt %, of LDH, by solution-intercalation method. The effect of LDH contents on thermal, physicomechanical, and morphological property of PVA films were investigated. Differential scanning calorimetric analysis reveals that LDH layers promote a new crystalline phase for PVA. The tensile analysis of PVA/LDH nanocomposites indicates reduction in tensile strength and modulus with change in LDH concentration and moisture. The micro-structure analysis by optical microscopy and scanning electron microscopy demonstrates exfoliation and dispersion of LDHs in the PVA matrix in a disorderly fashion. The primary focus of the present investigation is to explore the potential of LDHs as nanofiller in a polyhydroxy polymer without surface modification. © 2010 Wiley Periodicals, Inc. J Appl Polym Sci 116: 1671–1677, 2010

Key words: polymer-matrix composites; mechanical properties; differential scanning calorimetry; casting; poly(vinyl alcohol)

INTRODUCTION

Polymeric nanocomposites possess superior properties than that of conventional microsized filler composites due to the ultrafine dimension of the filler. Nanocomposites typically contain 1–5 wt % of filler loading depending on the ultimate properties to be achieved. Nanocomposites possess improved mechanical properties, gas barrier properties, and reduced flammability, increased heat distortion temperature, reduced solvent uptake, and lower flammability. The polymer nanocomposites could be obtained by using two different types of additives, one with particle size in the nanometer range and other with layered crystalline geometry. Layered double hydroxides (LDHs) also known as anionic or hydrotalcite, have a layered structure with the aspect ratio similar to or even higher than the ones observed for the aluminosilicate clays. The most remarkable aspect of LDH materials in comparison with various natural clay materials is their homogeneous composition, which allows compound designers to maintain the impurity level at minimum.

The dispersion of the nanoparticles within the polymer has significant influence on the properties of the material. In general, the hydrophilic nanoparticles are modified to make organophilic to get better dispersion in organophilic polymers.[1] However, it was found that the hydrophilic character of MMT clay promotes dispersion of these inorganic crystalline layers in water-soluble polymers such as poly(ethylene oxide)[2] and PVA.[3] More recently, PVA-based nanocomposites have been developed to improve PVA's properties and further explore its applications[4–7] by solution casting process. LDH-based nanocomposites prepared by solution casting process showed exfoliated nature of the dispersed particles.[8] Inspired from these studies, this work is focused on investigating the properties of PVA/LDH nanocomposites by solution casting method. PVA is a polyhydroxy polymer that has been studied intensively because of its good film forming character and physical properties, high hydrophilicity, processability, nontoxic, biocompatibility, biodegradability, and chemical resistance.[9]

In the ongoing efforts[10–12] to modify the PVA films, this study reports the preparation of PVA

nanocomposite films using LDH for the first time by solution-intercalation method. The primary focus of the present investigation is to explore the potential of LDH materials as filler in a hydrophilic polymer like PVA without modification. The LDH concentration of the composite was varied from 2 to 8 wt %. The properties of the PVA/LDH nanocomposites films were investigated by varying the LDH contents from 2 to 8 wt % using thermal analysis, physicomechanical properties, X-ray diffraction (XRD) analysis, optical microscopy (OM), and scanning electron microscopy (SEM).

EXPERIMENTAL

Materials

The polymer used in this study was PVA (weight average molecular weight of 1,25,000, degree of hydrolysis 80–90%, ash 0.75%) supplied M/s S.D. Fine Chem. Ltd, Mumbai, India. Anhydrous magnesium chloride and aluminum chloride, and urea were also supplied by M/s S.D. Fine Chem. Ltd, Mumbai, India. The PVA was kept in a sealed container to prevent moisture absorption before use.

Preparation of Mg-Al LDH

Mg-Al LDH was synthesized by urea hydrolysis method.[13] An aqueous solution containing Al^{3+} and Mg^{2+} with the molar fraction $Al^{3+}/(Al^{3+} + Mg^{2+})$ equal to 0.33 was prepared by dissolving $AlCl_3$ and $MgCl_2$ in distilled water. To this solution solid urea was added until the molar fraction, urea/$(Al^{3+} + Mg^{2+})$ reached 3.3. The clear solution was refluxed for 36 h. The white precipitate was then filtered, washed until chloride free and dried in vacuum at 60°C till constant weight and used for the preparation of nanocomposites.

Preparation of PVA/LDH nanocomposite films

Nanocomposites were prepared by a solution-intercalation film-casting method; films were cast from LDH water suspension where PVA was dissolved. PVA solution was blended with 2, 4, 6, and 8 wt % of LDH nanoparticles. The solid content of PVA and LDH was optimized at 7.5% in water and the system was made into a homogeneous solution by constant stirring at temperature of around 80–90°C for 30 min when the homogenization was obtained, polymer films were prepared by pouring the solution into glass plates (35×35 cm^2) and allowing the water to evaporate at room temperature. After drying, the films were removed from the mould and used for further studies.

Differential scanning calorimetry

Solution-casted nanocomposite films were analyzed by differential scanning calorimetry (DSC; DSC 2010, TA instruments, New castle, DE) to determine the PVA crystal properties from 50 to 250°C in nitrogen atmosphere at the heating rate of 10°C/min. The percentage of crystallinity (X_c) of the PVA component in the composite was obtained as follows:

$$X_c = \frac{\Delta H_f}{W \times H_{f,100\%}}$$

where ΔH_f and $\Delta H_{f,100\%}$ are the heats of fusion for 100% crystalline PVA and PVA, respectively. W is the weight fraction of PVA and $\Delta H_{f,100\%}$ was taken to be 163 J/g.[14]

X-ray diffraction analysis

XRD analysis over $2\theta = 4$–50°, in steps of 0.02° was carried out using Rigaku Miniflex diffractometer (40 kV, 10 mA) with Ni-filtered Cu Kα radiation (0.1542 nm), Japan. XRD spectra were interpreted with respect to the position of the basal peak, which depends on the distance between two adjacent metal hydroxide sheets in the LDH crystal lattice. The higher order peaks of the same hkl series were also reported as they indicate the presence of repeating crystal planes and symmetry in a specific crystallographic direction.

Physicomechanical properties

Among mechanical properties, the tensile strength is one of the most frequently used for comparison. In this experiment, tensile tests were performed on nanocomposite films (dried at 55°C for 2 h and on the samples equilibrated at 50 ± 5% RH and 23 ± 2°C) as per ASTM D 882 in universal testing machine manufactured using Lloyd Instruments, UK (Model LR 100K) with a cross-head speed of 50 mm/min. At least five specimens are examined in each group, the average is calculated, and reported. Tear strength measurements were made as per ASTM D 1992 in ATSFAAR Elmendorf Tear Tester (ATS 100, Italy) using films of size 63×76 mm^2. Burst strength measurements were made as per ASTM D774-67 in CIPET Burst strength tester(BST: A1 01) using films of size (6×6 cm^2). Moisture content was measured for the equilibrated samples in laboratory conditions. Density of the modified films was measured using Mettler PM200 electronic weighing balance as per ASTM D 792 displacement method. The solubility tests were carried out on dried film samples at 23 ± 2°C and 50 ± 5% RH. The optical micrographs were taken with OLYMBUS
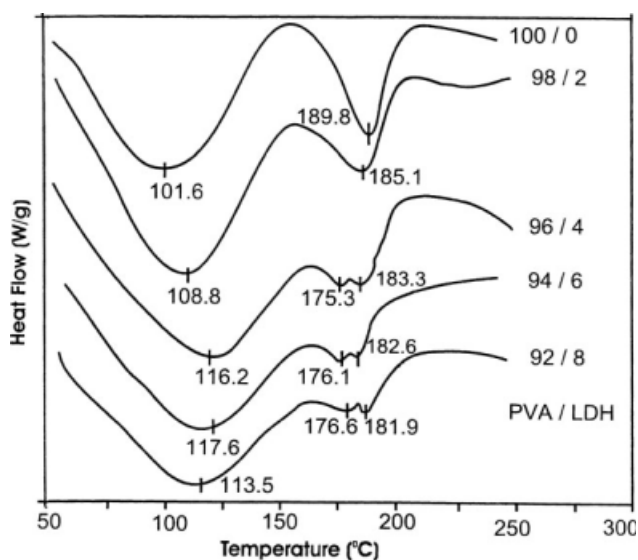
Figure 1 DSC thermograms of PVA/LDH nanocomposite films.

BX50 polarizing microscope equipped with a LINKAM THMS 600 heating stage and digital camera. SEM photograph of the LDH and PVA/LDH nanocomposites were observed on a JEOL (JSM-5800, Tokyo, Japan) with an acceleration voltage of 20 kV.

RESULTS AND DISCUSSION

Thermal analysis

The thermal properties of PVA/LDH nanocomposite films were investigated by DSC to analyze the effect of LDH content on glass transition temperature (T_g), melting temperature (T_m), heat-of-fusion and crystallinity of PVA films. The DSC thermograms of PVA and PVA/LDH films are shown in Figure 1 and the results are summarized in Table I. The incorporation LDH layers viz., 2, 4, 6, and 8 wt % into the PVA matrix increases the T_g of PVA from 101.6 to 113.5°C. Glass-transition process is considered to be affected by molecular packing, chain rigidity, and linearity.[15] An increase in T_g with increase in LDH

loading may be as a result of confinement effects and strong intercalations between polymer and filler particles. These intercalations, leading to restricted segmental mobility of the molecular chains in the vicinity of the LDH, retard the cooperative motions of the polymer chains and which leads to increase in T_g of at least part of the polymeric material. The observed increase in T_g of the PVA matrix is very similar to results observed in PVA/silica systems.[16,17] However, at higher loading, the absence of chain entanglements and the presence of excess free volume associated with the packaging constraints the intercalated chains. This would lead to a decrease in T_g. PVA is an atactic polymer material but exhibits crystallinity, as the hydroxyl groups are small enough to fit into the lattice without disrupting it. Majority of the commercially available grades of PVA are atactic and crystalline. PVA is somewhat special in that crystallization can occur in the atactic (no stereoregular) form. This is attributed to hydrogen atoms and hydroxyl groups (—OH) having roughly similar sizes, which allows the close regular packing of chains. Strong hydrogen bonding between the hydroxyl groups on neighboring chains also tend to hold the molecules in a regular structure in spite of the lack of stereoregularity. The introduction of nanosized fillers affects both crystallinity and the physical network causing variations in both T_g values and, in the melting enthalpy and temperature.

The neat PVA, which has melting temperature (T_m) at 189.8°C (Fig. 1, Table I), shows decrease in T_m from 189.8 to 181.9°C with increase in LDH contents from 0 to 8 wt %. This decrease in melting temperature might be related to a decrease in the crystallinity of the sample, and perfection of the crystal structure due to the inclusion of the filler in the crystalline regions of PVA. An additional melting peak appears in the melting region of composites containing 4, 6, and 8 wt % of LDHs, which is absent in the pure PVA. What was observed was a crystalline-phase separated system that exhibited a dual melting point. That dual melting point arose from two crystal phases: one formed primarily by

TABLE I
Thermal Properties of PVA/LDH Nanocomposite Films

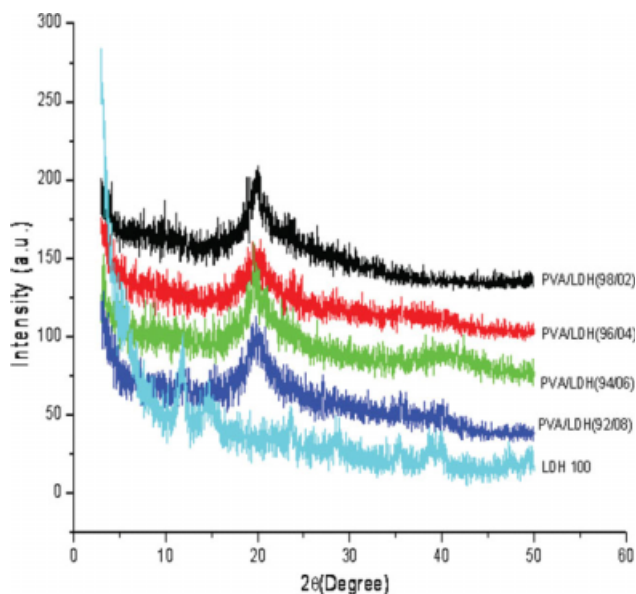| Composition weight (%)		Glass transition temperature (T_g) (°C)	Melting temperature (T_m) (°C)	Heat of fusion (ΔH) (J/g)	Percentage of crystallinity (X_c) (%)
PVA	LDH				
100	00	101.6	189.8	18.50	11.30
98	02	108.8	185.1	15.00	09.40
96	04	116.2	175.3, 183.3	10.49	06.70
94	06	117.6	176.1, 182.6	06.20	04.05
92	08	113.5	176.6, 181.9	05.57	03.72

Figure 2 XRD patterns of LDH, PVA/LDH (98/02), PVA/LDH (96/04), PVA/LDH (94/06), and PVA/LDH (92/08) nanocomposite films. [Color figure can be viewed in the online issue, which is available at www.interscience. wiley.com.]

syndiotactic sequences and the other primarily by atactic sequences. The two types of crystals have melting points that deferrer by about 5–8°C. The new crystal form grows linearly with the LDH concentration and at the expense of the bulk PVA crystal phase. This clearly suggests the low T_m phase is induced by the presence of LDH layers.

The study of the degree of crystallinity is very significant to understand the changes in the structural characteristics induced by LDH. To check whether the filler is located in the crystalline zones of the composite material, this study reports the dependence of the melting enthalpy and the degree of crystallinity on the filler content. Probably, the most widely used technique for estimating degree of crystallinity is by heat-of-fusion measurements from DSC. Table I shows the variation of melting enthalpy

as a function of the composition as measured by DSC. Apparently the value of melting enthalpy decreases gradually with increase of LDH content, indicating decrease in crystallinity. All the results indicate that the nanoparticles are distributed in the crystalline regions of PVA matrix. The crystalline order of PVA matrix is broken as a consequence of the formation of filler aggregates. PVA crystallinity decreased significantly from 11.3 to 3.72% (Table I).

X-ray diffraction analysis

The XRD analysis is used as a very useful method to describe the extent of intercalation and exfoliation of the nanofiller having layered structure. The complete or high degree of exfoliation of layered crystalline filler in polymer matrix certainly means disappearance of corresponding peaks from the XRD spectrum. The XRD spectrum of synthesized LDH and PVA/LDH nanocomposite films containing 2, 4, 6, and 8 wt % of LDH are shown in Figure 2. The XRD spectrum of synthesized Mg-Al LDH shows that the synthesized material has highly crystalline nature and layered geometry.[18] The position of the basal peak at $2\theta = 11.84$ indicates that the distance between two adjacent metal hydroxide sheets is about 0.76 nm. However, XRD pattern of PVA/LDH nanocomposites are characterized by the disappearance of the diffraction peaks corresponding to the LDH irrespective of the variation in LDH content. The only new broad diffraction peak appeared at $2\theta = 19.60$ corresponds to the PVA polymer matrix.[19,20] This complete disappearance of LDH peaks may be due to the partial exfoliated structure, in which the gallery height of intercalated layers is large enough and the layer correlation is not detected by X-ray diffractometer. Although XRD provides a partial picture about distribution of nanofiller and disappearance of peak corresponding to d-spacings does not always confirm the exfoliated nanocomposites, a complete characterization of nanocomposite morphology requires microscopic investigation.[21–23]

TABLE II
Tensile Properties of PVA/LDH Nanocomposite Films

| Tensile property		Weight percentage of LDH nanoparticles in PVA films				
		0	2	4	6	8
Load at beak (N)	Dried at 55°C for 2 h	159.30	107.20	105.70	92.58	86.97
	Equilibrated samples	86.23	81.14	62.05	57.46	55.19
Tensile strength	Dried at 55°C for 2 h	37.14	39.25	35.34	21.58	20.27
at break (N/mm^2)	Equilibrated samples	27.64	24.01	19.04	18.46	16.25
Tensile elongation	Dried at 55°C for 2 h	209.10	166.80	143.40	135.20	131.80
at break (%)	Equilibrated samples	180.40	203.30	213.40	218.50	222
Tensile modulus	Dried at 55°C for 2 h	923.00	1100.0	724.30	356	300
(N/mm^2)	Equilibrated samples	21.06	14.87	11.85	8.87	7.80
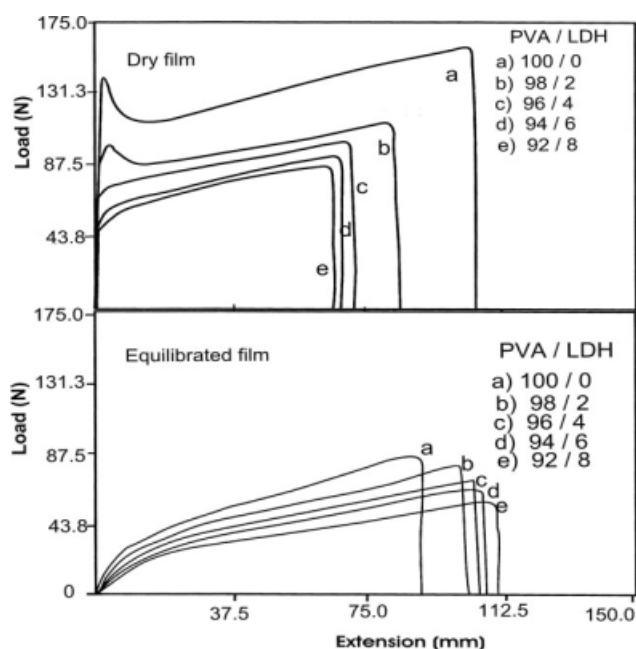
Figure 3 Stress–strain curves of dry and equilibrated PVA/LDH nanocomposite films.

Tensile properties of PVA/LDH nanocomposites

Tensile tests results of dry and equilibrated samples are summarized and shown in Table II. The tensile results reveal the effects of moisture, where dry films are having higher tensile strength and tensile modulus compared with the equilibrated sample containing moisture. Similarly, the LDH addition also has significant effect on tensile strength and modulus. For dry samples, the tensile strength at break decreased from 37.14 to 20.27 N/mm^2 and tensile modulus decreased from 923 to 300 N/mm^2 for the addition 2–8% LDH. For equilibrated samples, the tensile strength at break decreased from 27.64 to 16.25 N/mm^2 and tensile modulus decreased from 21.06 to 7.8 N/mm^2 for the addition 2–8% LDH. The stress–strain diagrams of dry and equilibrated PVA/LDH films are shown in Figure 3. The stress–strain curve of dry films (Fig. 3) shows neck formation (neat PVA film and PVA film with

2 wt % LDH) after yield point. The neck formation changed with increase in LDH content. The tensile load at break decreased from 159.3 to 86.97 N and tensile elongation at break decreased from 209.1 to 131.8% with increase in LDH content. PVA films with moisture (Fig. 3) does not show neck formation as in the case of dry films, where the tensile load at break decreased from 86.23 to 55.19 N and, however, tensile elongation at break increased from 180 to 222% with increase in LDH content. To rationalize these observations, it is appropriate to say that reduction in tensile load with consequent increase in percentage of nanoparticles may due to the plasticization effect of LDH on PVA matrix. Similar to hydroxyl groups of PVA, hydroxyl groups of LDH also absorb moisture. In summary, it is the presence of hydroxyl groups in nanoparticles and moisture that dominates the mechanical behavior. This trend is similar to the systems containing gelatinized starch, in which moisture content has a large effect on mechanical properties. The tensile strength of unplasticized PVA depends on the moisture content and relative humidity. The tensile modulus of dried samples is very high when compared with equilibrated samples. However, the tensile modulus decreased with increase in filler loading from 2, 4, 6, and 8 wt %. For dried samples, initially there was an increase in tensile modulus, but higher loading decreases the modulus. This may be due to the poor dispersion of filler particles.

Tear and burst strength

Tear and burst strength results of the films are shown in the Table III. From the table, it is clear that the internal tear resistance of neat PVA decreased from 503 gf to 435 gf with the addition of LDH nanoparticles. The burst strength of PVA film decreased from 94 to 67 psi with increase in LDH content from 0 to 8 wt %. The burst strength is a measure of overall strength of the film. The decrease in tear and burst strength may be due to the

TABLE III
Effects of LDH Nanoparticles on Moisture, Burst, Tear Strength, and Density of PVA/LDH Nanocomposite Films

Composition weight (%)		Moisture content (%)	Burst strength (psi)	Tear strength (gf)	Density (g/cc)
PVA	LDH				
100	00	07.73	94	503	1.236
98	02	07.90	88	518	1.270
96	04	09.10	80	520	1.270
94	06	10.50	70	521	1.275
92	08	12.32	67	435	1.577

TABLE IV
Effect of LDH Nanoparticles on Solubility of PVA/LDH Nanocomposite Films

Composition weight (%)		Dissolution time (min)					
PVA	LDH	Water	DMSO	DMF	Glycerol	Xylene	CCl$_4$
100	00	15	30	Swelling	Swelling	No change	No change
98	02	20	40	Swelling	Swelling	No change	No change
96	04	30	50	Swelling	Swelling	No change	No change
94	06	40	70	Swelling	Swelling	No change	No change
92	08	45	85	Swelling	Swelling	No change	No change

DMSO, dimethyl sulfoxide; DMF, dimethyl formamide; CCl$_4$, carbon tetrachloride.

particulate nature of nanoparticle, which does not support the tear and burst strengths.

Moisture content and density

The moisture content of PVA and its LDH nanocomposite films are shown in Table III, from the table, it is clear that the filler loading increases the moisture content from 7.73 to 12.32%. The increase in moisture content may be either due to the enhanced hydrophilicity of LDH or reduction in percentage of crystallinity of PVA or both. The density value of PVA/LDH films shows gradual increases from 1.236 to 1.577 g/cc with filler loading (Table III).

Solubility resistance and swelling analysis

The PVA/LDH nanocomposite films were tested for its resistance in water, dimethyl sulfoxide (DMSO), dimethyl formamide (DMF), glycerol, xylene, and carbon tetrachloride (Table IV). The films lost their strength and became soluble in water, and DMSO. Dissolution time of these films in water and DMSO increased with increase in LDH content, this increase in dissolution may be due to the strong interaction and formation of complex structure between PVA and LDH. However, the PVA/LDH shows only swelling in DMF and glycerol, and remains virtually unaffected by hydrocarbons (xylene) and chlorinated hydrocarbons (carbon tetrachloride).

Surface morphology

OM is used to elucidate the dispersion behavior of the LDH layers in the PVA matrix. More direct evidence for the filler dispersion in the composite was provided by the micrographics analysis of cast films (Fig. 4). The optical micrographs of PVA nanocomposite films containing 2, 4, 6, and 8 wt % of LDH sheets are shown in Figure 4(a–d), respectively. Optical micrograph of PVA/LDH composite reveals a very complex morphology of the dispersed particles, which vary widely in shape and size. Figure 4

shows the presence of single LDH layers, orderly stacked LDH layers, and LDH aggregates. The OM shows the presence of single LDH sheets in form strips. The results demonstrate that the LDH layers lost their ordered stacking structure and were dispersed in PVA matrix. Same figure contains substantial strongly oriented orderly stacked LDH layers and aggregate/agglomerates. All the three categories of LDH nanoparticles, like single LDH sheet, orderly stacked LDH sheets, and aggregate/agglomerates are all seen in all the figures. However, the presence of single sheets and orderly stacked sheets decrease with increase of LDH percentage from 2 to 8 wt % and aggregate/agglomerates increases. In summary, it could be said that irrespective of the LDH concentration, PVA/LDH composites show the presence single LDH layers, orderly stacked LDH layers, and LDH aggregates in all compositions.
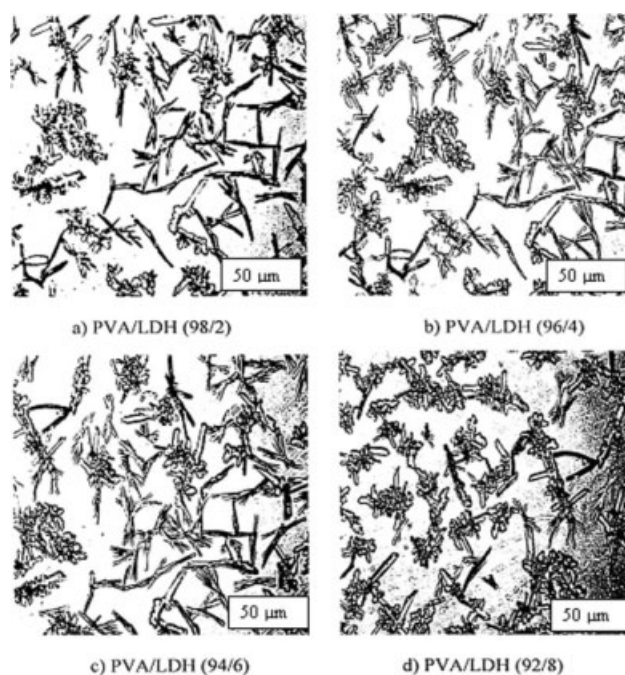

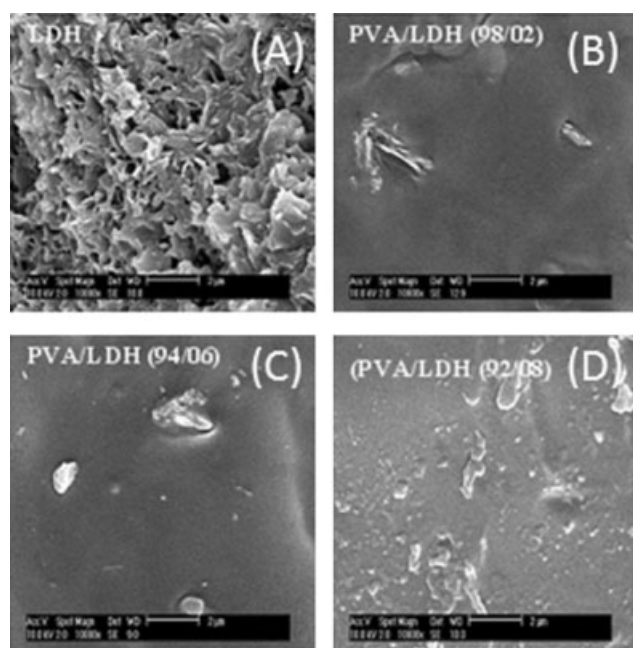**Figure 4** Optical photomicrographs of PVA/LDH nanocomposite films.

Figure 5 SEM micrographs of LDH, PVA/LDH (98/02), PVA/LDH (96/04), PVA/LDH (94/06), and PVA/LDH (92/08) nanocomposite films.

The scanning electron micrograph of pure LDH, and PVA/LDH nanocomposites containing different amounts of LDH nanoparticles are shown in Figure 5. The SEM image of pure LDH [Fig. 5(A)] reveals the nature of LDH particles before solution blending, which roughly consists of plate-like shape stacked on top of each other with lateral dimensions ranging over few micrometer and thickness over few hundreds nanometer. The SEM images of nanocomposite films do not give clarity on the dispersion of LDH nanoparticles in the PVA matrix and further increase in LDH content increases the agglomeration of LDH nanoparticles in the PVA matrix. Apparently, it seems that the particles are distributed uniformly in the polymer matrix.

CONCLUSIONS

PVA and Mg-Al LDH nancomposite films have been prepared with various LDH concentrations by solution intercalation process. DSC analysis shows that the introduction of LDH platelets has caused the formation of a different type of crystal structure in the interphase region. These nanoscale process, driven by the physical and chemical nature of the LDH pla-

telets, affect the final macroscopic properties of the nanocomposites, such as thermal and mechanical properties. The mechanical properties of the composites were changed drastically due to moisture and change in concentrations of LDH. Overall, the LDH content in the polymer matrix affects both the crystallinity and the mechanical properties especially the tensile properties. The presence of single LDH sheets in form strips in optical micrographs shows the dispersion LDH nanoparticles in PVA matrix.

References

1. Ebdon, J. R.; Hunt, B.; Joseph, P. J. Polym Degrad Stab 2004, 83, 181.
2. Vaia, R. A.; Vasudevan, S.; Krawiec, W.; Scanlon, L. G.; Giannelis, E. P. J Polym Sci Part B: Polym Phys 1997, 35, 59.
3. Carrado, K. A.; Thiyagarajan, P.; Elder, D. L. Clays Clay Miner 1996, 44, 506.
4. Nakane, K.; Yamashita, T.; Iwakura, K.; Suzuki, F. J Appl Polym Sci 1999, 74, 133.
5. Yeun, J.-H.; Bang, G.-S.; Park, B. J.; Ham, S. K.; Chang, J.-H. J Appl Polym Sci 2006, 101, 591.
6. Alla, S.G.A.; El-Din, H. M. N.; El-Naggar, A. W. M. J Appl Polym Sci 2006, 102, 1129.
7. Chang, J.-H.; Jang, T.-G.; Ihn, K. J.; Lee, W.-K.; Sur, G. S. J Appl Polym Sci 2003, 90, 3208.
8. Husich, H. B.; Chen, C. Y. Polymer 2000, 44, 5275.
9. Krumova, M.; Lopez, D.; Benavente, R.; Mijangos, C.; Parena, J. M. Polymer 2000, 41, 9265.
10. Ramaraj, B.; Radhakrishnan, G. Polymer 1994, 35, 2167.
11. Ramaraj, B. J Appl Polym Sci 2007, 103, 1127.
12. Ramaraj, B. J Appl Polym Sci 2007, 103, 909.
13. Costa, F. R.; Abdel-Goad, M.; Wagenknecht, U.; Heinrich, G. Polymer 2005, 46, 4447.
14. James, R.; Runt, P. Crystallinity Determination, Encylopedia of Polymer Science and Engineering, 2nd ed.; Wiley: New York, 1986; Vol. 4, p 487.
15. Li, F.; Ge, J.; Honigfort, P.; Tang, S.; Cheng, J.; Harris, F.; Cheng, S. Polymer 1999, 40, 4987.
16. Peng, Z.; Kong, L. X.; Li, S.-D. J Appl Polym Sci 2005, 96, 1436.
17. Chen, Y.; Zhou, S.; Yang, H.; Wu, L. J Appl Polym Sci 2005, 95, 1032.
18. Costantino, U.; Marmottini, F.; Rocchetti, M.; Vivai, R. Eur J Inorg Chem 1998, 1439, 1446.
19. Qian, X. F.; Yin, J.; Guo, X. X.; Yang, X. F.; Zhu, Z. K.; Liu, J. J Mater Sci Lett 2000, 19, 235.
20. Wang, H.; Fang, P.; Chen, Z.; Wang, S. Appl Surf Sci 2007, 253, 8495.
21. Yu, Z. Z.; Yang, M.; Zhang, Q.; Zhao, C.; Mai, Y. W. J Polym Sci Part B: Polym Phys 2003, 41, 1234.
22. Wang, K.; Liang, S.; Du, R.; Zhang, Q.; Fu, Q. Polymer 2004, 45, 7953.
23. Morgan, A. B.; Gilman, J. W. J Appl Polym Sci 2003, 87, 1329.